



# Insight into the role of $\text{Ti}^{3+}$ in photocatalytic performance of shuriken-shaped $\text{BiVO}_4/\text{TiO}_{2-x}$ heterojunction



Yunqing Zhu<sup>a,\*</sup>, Muhammad Wajid Shah<sup>a,b,1</sup>, Chuanyi Wang<sup>a,\*</sup>

<sup>a</sup> Laboratory of Environmental Sciences and Technology, Xinjiang Technical Institute of Physics & Chemistry, Key Laboratory of Functional Materials and Devices for Special Environments, Chinese Academy of Sciences, Urumqi 830011, China

<sup>b</sup> University of Chinese Academy of Sciences, Beijing, 100049, China

## ARTICLE INFO

### Article history:

Received 8 August 2016

Received in revised form 13 October 2016

Accepted 18 October 2016

Available online 19 October 2016

### Keywords:

Heterojunction

$\text{BiVO}_4/\text{TiO}_{2-x}$

$\text{Ti}^{3+}$  doping

Photocatalysis

Band alignment

## ABSTRACT

Heterojunction is recognized as an effective approach to improve photocatalytic performance, but a well-matched energy band alignment is critical therein. In this work, the shuriken-shaped  $\text{BiVO}_4/\text{TiO}_{2-x}$  heterojunction is built by engineering the electronic structure of  $\text{TiO}_2$  with  $\text{Ti}^{3+}$  self-doping via a two-step hydrothermal process to achieve a high photocatalytic performance. The presence of  $\text{Ti}^{3+}$  creates a defect energy level under the conduction band of  $\text{TiO}_2$ , and thereby diminishes the interfacial energy barrier between  $\text{BiVO}_4$  and  $\text{TiO}_2$ . The  $\text{Ti}^{3+}$  defect energy level promotes the electron transfer from  $\text{BiVO}_4$  to conduction band of  $\text{TiO}_{2-x}$ . The test of phenol degradation under 300 W Xenon lamp equipped with UV cut-off filter ( $\lambda \geq 420$  nm) demonstrates that  $\text{BiVO}_4/\text{TiO}_{2-x}$  heterojunction exhibits higher photocatalytic activity than its counter parts, pure  $\text{BiVO}_4$  and the physis mixture of  $\text{BiVO}_4$  and  $\text{TiO}_{2-x}$ . The improved photocatalytic performance is mainly attributed to the heterojunction formed between  $\text{BiVO}_4$  and  $\text{TiO}_{2-x}$ , which improves the separation of photogenerated charge carriers as support by comparative photocurrent and time-resolved PL spectral measurements. In addition,  $\text{Ti}^{3+}$  self-doping also narrows the bandgap of  $\text{TiO}_2$  and enhances the visible-light activity of  $\text{TiO}_2$ . The holes of  $\text{TiO}_{2-x}$  transfer to the valance band of  $\text{BiVO}_4$  which further significantly improves the separation of photogenerated charge carriers, further. Additionally, the high surface area caused by  $\text{TiO}_{2-x}$  also contributes to the improved photocatalytic efficiency.

© 2016 Elsevier B.V. All rights reserved.

## 1. Introduction

Photocatalysis has received considerable attention for its potential application in many fields, such as environmental remediation using solar energy [1–3]. Various metal oxides have been widely studied as candidate materials for photocatalysis because of their stability and relative abundance.  $\text{BiVO}_4$  is recognized as one of the promising photocatalysts, owing to its excellent stability against photocorrosion and chemical corrosion, narrow bandgap ( $\sim 2.4$  eV) in the monoclinic phase, and low cost [4–6]. The direct narrow bandgap makes  $\text{BiVO}_4$  as a good light absorber, but its carrier diffusion length ( $L_d$ ) around  $70\text{ nm}^3$  is relatively short due to a high recombination rate of charge carriers [7], which becomes a main factor that restricts its practical applications. Additionally, low sur-

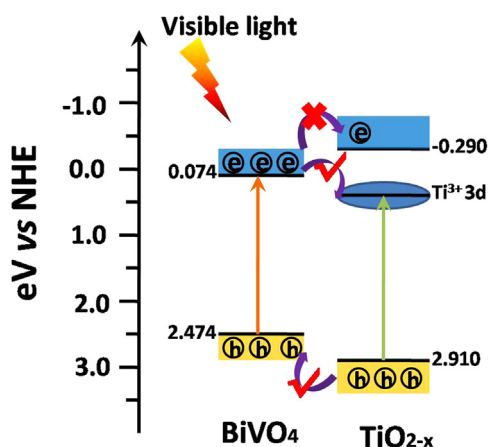
face area and weak surface adsorption ability of micron-sized  $\text{BiVO}_4$  are also important issues that strongly limit its application.

To overcome the above stated shortcomings of  $\text{BiVO}_4$ , various strategies including nanostructure fabrication, heterojunction and surface modification have been explored [8,9]. Among these strategies, heterojunction construction is proposed as one of the most effective approaches to overcome the barrier of charge transfer [10,11]. The built-in electric field formed in the heterojunctions makes the photo generated electrons and holes move into opposite directions, thus prolonging the lifetime of the carriers. The noble metals (such as Ag, Au, or Pt), the carbon nano-materials (graphene) and the semiconductors (such as  $\text{TiO}_2$ ,  $\text{WO}_3$ ,  $\text{CeO}_2$ ,  $\text{Bi}_2\text{WO}_6$ , and CdS) are widely adopted for combining with  $\text{BiVO}_4$  to achieve a high efficiency in photocatalysis performance [12–17]. Among these materials,  $\text{TiO}_2$  [18,19] is one of the most representative photocatalysts.  $\text{TiO}_2$  is proved to be a promising photocatalyst due to its practicality and strong photocatalytic oxidation capacity [20]. But its wide band gap ( $\sim 3.2$  eV) [21] limits its light absorption to UV range. Therefore, combining of  $\text{TiO}_2$  with  $\text{BiVO}_4$  could be a potential pathway not only to extend the light absorption of

\* Corresponding authors.

E-mail addresses: [zhuyq@ms.xjb.ac.cn](mailto:zhuyq@ms.xjb.ac.cn) (Y. Zhu), [cywang@ms.xjb.ac.cn](mailto:cywang@ms.xjb.ac.cn) (C. Wang).

<sup>1</sup> These authors contributed equally to this work.



**Scheme 1.** Relative energy band levels of BiVO<sub>4</sub> and TiO<sub>2-x</sub> heterojunction by self-doping of Ti<sup>3+</sup>.

TiO<sub>2</sub> to visible range, but also to enhance the transfer of charge carriers by forming heterojunction at the interface. However, the energy band matching is a key factor for achieving a highly effective BiVO<sub>4</sub>/TiO<sub>2</sub> heterojunctions. It is known that the conduction band of anatase TiO<sub>2</sub> is  $-0.290$  eV vs NHE, [22] while for monoclinic BiVO<sub>4</sub>, it is  $0.074$  eV vs NHE [23]. As a result, when the BiVO<sub>4</sub>/TiO<sub>2</sub> heterojunction is formed, an interfacial energy barrier is present in the interface. Therefore, under visible light irradiation, it is impossible for the generated electrons of BiVO<sub>4</sub> to climb over the energy barrier migrating to the conduction band of TiO<sub>2</sub>. The unmatched energy band alignment critically affects the charge carrier migration in the formed BiVO<sub>4</sub>/TiO<sub>2</sub> heterojunctions, which is one of the reasons for very limited success achieved in this regard.

In our previous work, various strategies were developed to introduce a defect electronic band in TiO<sub>2</sub> by self-doping of Ti<sup>3+</sup> in the TiO<sub>2</sub> lattice [24–26]. The location of Ti<sup>3+</sup> induced electronic band is below the conduction band of TiO<sub>2</sub> [27,28] as illustrated in Scheme 1, which reduces the interfacial energy barrier between BiVO<sub>4</sub> and TiO<sub>2</sub>, and makes it possible for the migration of electrons from BiVO<sub>4</sub> to the conduction band of TiO<sub>2</sub> (Scheme 1). The Ti<sup>3+</sup> in TiO<sub>2</sub> matrix can also trigger the visible-light activity of TiO<sub>2</sub> [29–32]. On the other hand, the generated holes of TiO<sub>2</sub> can also transfer to the valance band of BiVO<sub>4</sub>. In addition, the TiO<sub>2-x</sub> prepared according to our previous work exhibits extremely high surface area ( $263.95 \text{ m}^2 \text{ g}^{-1}$ ) [24], which could provide abundant reactive sites for photocatalytic reaction. As supported by the test of photo degrading phenol, the construction of heterojunctions between BiVO<sub>4</sub> and TiO<sub>2-x</sub> is an effective approach towards high photocatalytic performance.

## 2. Experiment section

### 2.1. Material preparation

The BiVO<sub>4</sub> and TiO<sub>2-x</sub> heterojunction was prepared via a two-step hydrothermal process and denoted as BiVO<sub>4</sub>/TiO<sub>2-x</sub>. Typically, the shuriken-shaped BiVO<sub>4</sub> samples were synthesized using an aqueous solution of NH<sub>4</sub>VO<sub>3</sub> (6 mM) and Bi(NO<sub>3</sub>)<sub>3</sub>·5H<sub>2</sub>O (6 mM) in 2 M HNO<sub>3</sub> (30 mL) at room temperature, with addition of 100  $\mu\text{L}$  TiCl<sub>3</sub> solution (20%) as a structure directing agent [33]. The pH of the solution was adjusted to 5 with ammonia (28 wt.%) under vigorous stirring. The obtained mixture was transferred to a Teflon stainless steel autoclave and aged at 180 °C for 12 h. The yellow product of BiVO<sub>4</sub> was filtered and washed with plenty of distilled water/ethanol, and dried at 80 °C overnight.

The yellow BiVO<sub>4</sub> powder (0.25 g) was dispersed in water under ultrasonic to form suspension A. Different amounts (0, 0.9, 1.8, 2.2 and 3.6 mmol) of TiCl<sub>3</sub> (20% in HCl solution) and 0.7 g L-ascorbic acid were dissolved in water, and adjusted the pH to 4 by NaOH to form solution B. The solution B was subsequently added to suspension A and stirred for another 60 min. The mixture was then transferred to Teflon stainless steel autoclave and heated at 180 °C for 12 h. The obtained precipitates were collected by centrifugation and rinsed with plenty of distilled water/ethanol. After drying at 80 °C overnight, the materials were collected and labelled as BiVO<sub>4</sub>/TiO<sub>2-x</sub>(X) where X means the amount of Ti(III) precursor.

### 2.2. Material characterization

The morphologies and the particle sizes of as-prepared BiVO<sub>4</sub>/TiO<sub>2-x</sub>(X) samples were examined by scanning electron microscope (SEM) (FE-SEM, Zeiss Supra55vp, Germany). High resolution transmission electron microscopy (HRTEM) characterization was performed on a JEOL-JEM-2100 electron microscope. X-ray diffraction (XRD) patterns of the samples were collected on a Bruker D8 Advance powder diffractometer over scattering angles from 20° to 80° using Cu K $\alpha$  radiation. Absorption spectra analysis was conducted with a Shimadzu SolidSpec-3700DUV spectrophotometer equipped with diffuse reflectance attachment in a spectraloncoated integrating sphere against spectralon reference. Nitrogen adsorption/desorption isotherms were measured at 77 K on a surface area and porosity analyser (Quantachrome Instruments version 3.0). X-ray photoelectron spectra (XPS) of the samples were measured using a Kratos Analytical AMICUS XPS instrument. The Bruker Vertex 70 FT-IR spectrometer was utilized to record FT-IR spectra. The electron paramagnetic resonance (EPR) spectra were recorded by a Bruker E500 Spectrometer. Photoluminescence spectra (PL) were obtained by a fluorescence spectrophotometer (F-7000 FL Spectrophotometer) with a 150 W Xenon lamp as the excitation source at room temperature. The time-resolved PL measurements were performed on a Horiba Fluorolog-3 Spectrofluorometer using the time-correlated single photo counting (TCSPC) method for lifetime measurements, and the film samples were photoexcited using a 450 W X-lamp at wavelength of 340 nm.

### 2.3. Photocatalytic activity measurement

The photocatalytic activity of as prepared samples was evaluated by a model reaction, i.e., degradation of phenol under visible light. Typically, 40 mL of phenol solution ( $20 \text{ mg L}^{-1}$ ) in 50 mL quartz photo-reactor was employed for test.  $0.5 \text{ g L}^{-1}$  photocatalyst was dispersed into the phenol solution at neutral pH. The solution was stirred in dark for 40 min to obtain adsorption-desorption equilibrium and then irradiated by 300 W Xenon lamp equipped with UV cut-off filter ( $\lambda \geq 420 \text{ nm}$ ) at room temperature. 2 mL of aliquots were taken out at given time intervals and centrifuged to remove the photocatalysts particles before analysis of phenol concentration by Thermo Fisher Ultra 3000 HPLC equipped with a 25 cm  $\times$  4.6 mm Cosmosil C18 column.

The photo-electrochemical analysis was carried out with a CHI660E instrument using a three-electrode system. 50 mg of a sample photocatalyst was loaded on conductive surface of ITO glass and 0.05 M Na<sub>2</sub>SO<sub>4</sub> solution was used as electrolyte. 300 W Xenon lamp equipped with UV cut-off filter ( $\lambda \geq 420 \text{ nm}$ ) was used as a light source, and standard calomel electrode (SCE) was employed as reference electrode and Pt slice as counter electrode.

## 3. Result and discussion

Fig. 1 depicts the morphology of BiVO<sub>4</sub> and the BiVO<sub>4</sub>/TiO<sub>2-x</sub>(1.8 mmol) heterojunction. As shown in Fig. 1a,

Download English Version:

<https://daneshyari.com/en/article/6454515>

Download Persian Version:

<https://daneshyari.com/article/6454515>

[Daneshyari.com](https://daneshyari.com)